

Stability of C₆₀ fullerite intercalation compounds

Yang Wang and David Tománek

*Department of Physics and Astronomy and Center for Fundamental Materials Research,
Michigan State University, East Lansing, Michigan 48824-1116*

George F. Bertsch

*Department of Physics and Astronomy and National Superconducting Cyclotron Laboratory,
Michigan State University, East Lansing, Michigan 48824-1116*

Rodney S. Ruoff

SRI-International, 333 Ravenswood Avenue, Menlo Park, California 94025

(Received 12 June 1992)

We construct a thermodynamic Born-Haber cycle to predict formation energies of donor- and acceptor-based C₆₀ fullerite intercalation compounds with different stoichiometries. Energies associated with the individual steps in the cycle contain important related information such as the lattice constant, bulk modulus, and phonon spectra of the compounds. Our results indicate that alkali and alkaline-earth intercalated fullerite compounds are most stable.

I. INTRODUCTION

The successful bulk synthesis of fullerite,¹ a fcc crystal based on the icosahedral C₆₀ structure,² has opened an interdisciplinary field of "fullerene science" which cuts across physics, chemistry, and engineering. Perhaps the most exciting property of C₆₀ fullerite is superconductivity which occurs in the doped compound. Following the discovery of superconductivity in K₃C₆₀ with a transition temperature $T_c=18$ K,³ compounds have been synthesized using a variety of intercalants,^{4,5} yielding critical temperatures as high as 33 K in Cs₂RbC₆₀.⁶ While T_c values of doped fullerite are still below those found in high- T_c perovskite superconductors,⁷ intercalated fullerite shows superior materials properties and hence bears the higher potential for applicability. The intercalation process and the rigid-band behavior of intercalated fullerite resembles in many ways the extensively studied graphite intercalation compounds.⁸

The crucial property of fullerite intercalation compounds A_xC₆₀ is their stability against decomposition into the components in the standard state, i.e., C₆₀ (solid) and A (solid). The formation enthalpy is of interest not only for the donor compounds mentioned above, but also for potential acceptor compounds. This quantity is hard to calculate, since cohesion in these ionic compounds is dominated by a large Madelung energy.^{9,10} Still, even a rough estimate of the formation enthalpies across the Periodic Table is useful when considering the synthesis of C₆₀-based materials. The difficulty of obtaining a reliable value for the formation enthalpy is best illustrated by the spread of *ab initio* values for the formation enthalpy of K₃C₆₀ from K metal and bulk C₆₀, ranging from $\Delta H_f^0 = -1.7$ eV per K atom¹¹ to $\Delta H_f^0 = -6.6$ eV,¹² indicative of an extremely exothermic intercalation process.

The approach we use in the present paper is to de-

compose the formation process of fullerite intercalation compounds into well-defined steps and to estimate the energy involved in each step across the Periodic Table. These steps are combined into a thermodynamic Born-Haber cycle which determines the formation enthalpy. The prerequisite for this calculation is a detailed knowledge of the structure, lattice constant, and compressibility. Since this information is not available for most of the systems discussed here, we calculate these properties, together with the phonon structure, for the compounds of interest first. This is interesting information on its own merit and will be presented together with the calculated formation energies.

The paper is organized as follows. In Sec. II, we introduce the Born-Haber cycle used in the calculation. Our results for the structural and cohesive properties of fullerite intercalation compounds are given in Sec. III. In Sec. IV, we discuss our results. In Sec. V, we summarize our results and present conclusions.

II. BORN-HABER CYCLE

The formation enthalpy ΔH_f^0 at $T = 0$ K of A_nC₆₀ is defined by

$$nA(\text{solid}) + C_{60}(\text{solid}) \xrightarrow{n\Delta H_f^0} A_nC_{60}(\text{solid}). \quad (1)$$

If ΔH_f^0 is negative, the compound A_nC₆₀ is stable against decomposition into the pure components, namely the intercalant A in its solid form, A (solid), and pure fullerite, C₆₀ (solid). We determine ΔH_f^0 by formally decomposing the formation process of a fullerite intercalation compound into several physically well defined steps and evaluating the energies involved in the individual steps. This procedure, known as the Born-Haber cycle, has been used to determine reaction enthalpies of complex multistage reactions. The cycle for the formation of the donor com-

pound A_3C_{60} is illustrated in Fig. 1(a).

The first step involves the separation of the reference system into individual A atoms and C_{60} molecules, taking into account that 3 A atoms occur in the formula unit of the doped solid. The energy involved in this step is the cohesive energy of A, $3E_{\text{coh}}(A)$, and the binding energy of a C_{60} molecule in C_{60} (solid), $E_{\text{coh}}(C_{60} \text{ solid})$. In the next step, we consider the ionization of the three A atoms and the charge transfer to the C_{60} molecule. Here we have implied that C_{60} can act as electron acceptor; the electron affinity of the C_{60} molecule will be discussed later. This step requires the energy $3I(A)$, $I(A)$ being the ionization energy of the A atom. The three electrons are transferred from the donor atoms to the C_{60} molecule and release the energy $A_{\text{tot}} = A(C_{60}) + A(C_{60}^-) + A(C_{60}^{2-})$, where A is the electron affinity. In the last step, the A^+ and C_{60}^{3-} ions are combined to form the solid, thereby releasing the formation energy $E_{\text{coh}}(A_3^+C_{60}^{3-})$. Hence, the total energy gain during the formation of the $A_3^+C_{60}^{3-}$ system is

$$\Delta H_f^0 = 3E_{\text{coh}}(A) + E_{\text{coh}}(C_{60}) + 3I(A) - A(C_{60}) - A(C_{60}^-) - A(C_{60}^{2-}) - E_{\text{coh}}(A_3^+C_{60}^{3-}). \quad (2)$$

The relatively low ionization potential of C_{60} makes it a potential electron donor, raising the question about the stability of acceptor-intercalated fullerite. The Born-Haber cycle for the formation of the acceptor compound A_3C_{60} is illustrated in Fig. 1(b). It differs from the former one in the direction of charge transfer between the intercalant and the matrix. The electron affinity $A(A)$ of the intercalant and the ionization potentials of multiply charged C_{60} clusters, $I(C_{60}^{n+})$, are required in this step. The formation energy of the compound from the ions, $E_{\text{coh}}(A_3^-C_{60}^{3+})$, is defined with respect to the appropriately charged ions, and is given by

$$\Delta H_f^0 = 3E_{\text{coh}}(A) + E_{\text{coh}}(C_{60}) - 3A(A) + I(C_{60}) + I(C_{60}^+) + I(C_{60}^{2+}) - E_{\text{coh}}(A_3^-C_{60}^{3+}). \quad (3)$$

When evaluating the formation enthalpy using the Born-Haber cycle, we approximated each step by the corresponding energy and hence have neglected the contributions of nonzero temperature and pressure to ΔH_f^0 , which we estimate to be of the order of $\lesssim 0.1$ eV. Pre-

cise experimental data exist for the cohesive energies $E_{\text{coh}}(A)$,¹³ the ionization potentials $I(A)$, and electron affinities $A(A)$ across the Periodic Table.^{14,15} Unfortunately, no reliable experimental values exist for the binding energy of a C_{60} molecule in single crystals of C_{60} , and *ab initio* techniques tend to underestimate the weak Van der Waals binding between the C_{60} clusters.¹⁶ Therefore, we estimate this quantity in the close-packed fullerite lattice using a pair bond model as $E_{\text{coh}}(C_{60} \text{ solid}) = 6D(C_{60} - C_{60})$. The distance dependence of the pair potential $D(C_{60} - C_{60})$ is given by the Morse form

$$D(r) = D_e[(1 - e^{-\beta(r-r_e)})^2 - 1], \quad (4)$$

where D_e is the the dissociation energy of a pair of C_{60} molecules and r_e is their nearest-neighbor distance, and where β describes the distance dependence of the C_{60} - C_{60} interaction. We use $r_e = 10.04 \text{ \AA}$,¹⁷ $\beta = 0.866 \text{ \AA}^{-1}$, and $D_e = 0.8 \text{ eV}$ based on a combination of our previous calculation for the C_{60} solid¹⁸ and experimental data.¹⁹ Recent experimental data suggest a smaller value $E_{\text{coh}}(C_{60} \text{ solid}) = 1.76 \text{ eV}$ (at $T = 0 \text{ K}$) for polycrystalline C_{60} films.²⁰ As we will show later on, an accurate value of the cohesive energy is not crucial for the stability of the compounds since it is partly or mostly compensated in the formation of the compound with the same fcc crystal structure. It only has a small influence on the formation energy of the A_6C_{60} phase with a bcc structure, and a small inaccuracy in $E_{\text{coh}}(C_{60} \text{ solid})$ will not reverse the conclusions we draw.

We use the experimental results for the electron affinity of neutral C_{60} , $A(C_{60}) = 2.74 \text{ eV}$,²¹ and the ionization potential $I(C_{60}) = 7.54 \pm 0.04 \text{ eV}$.²² We note that the electron affinity of C_{60} is only slightly smaller than that of the electronegative elements in group VIIA, which makes the C_{60} molecule a good electron acceptor. On the other hand, the ionization potential of the C_{60} molecule lies close to that of electropositive Mg, which makes the C_{60} molecule a good electron donor as well. When calculating the higher electron affinities and ionization potentials, we modify the above values by the electrostatic energy which occurs during the attachment or detachment of electrons from a charged sphere with the C_{60} molecule radius $R = 3.5 \text{ \AA}$. The calculated total ionization potentials and electron affinities are summarized in Tables I and II. These estimates are in good general agreement

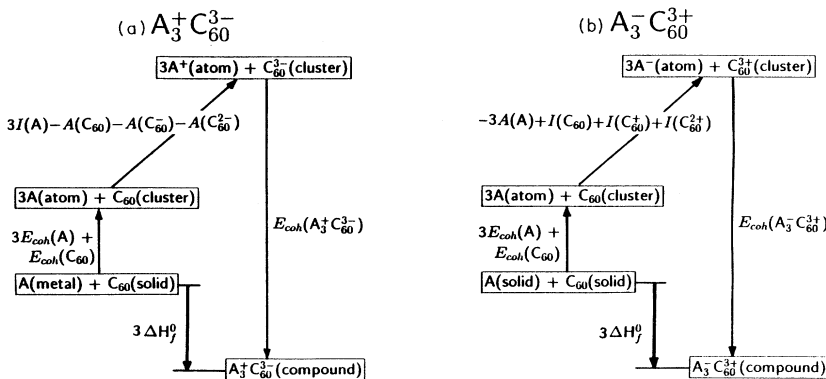


FIG. 1. Born-Haber cycle used to predict the formation enthalpy ΔH_f^0 of (a) donor and (b) acceptor C_{60} fullerite intercalation compounds.

TABLE I. Total ionization energy I_{tot} corresponding to the process $\text{C}_{60} \rightarrow \text{C}_{60}^{n+} + ne^-$.

Final-state configuration	C ₆₀ ⁺	C ₆₀ ²⁺	C ₆₀ ³⁺	C ₆₀ ⁶⁺	C ₆₀ ¹²⁺
I_{tot} (eV) ^a	7.54 ^b	19.20 19.00 ^c	34.96	106.98	362.07

^aThe first line contains data used in our calculation.

^bExperimental value of Ref. 22 based on photoionization.

^cExperimental value of Ref. 23 based on photoionization.

with available experimental data of Refs. 23–26. In particular, there is experimental evidence for a linear dependence of the ionization potentials and electron affinities on the final-state charge.²⁷

The formation energy $E_{\text{coh}}(\text{A}_n^+\text{C}_{60}^{n-})$ of the intercalation compound from the ions depends strongly on the structure. Here, we consider the AC₆₀ and A₃C₆₀ solid with the fcc structure, and the A₆C₆₀ solid with the bcc structure.⁹ $E_{\text{coh}}(\text{A}_n^+\text{C}_{60}^{n-})$ can be decomposed into three terms,

$$-E_{\text{coh}}(\text{A}_n^+\text{C}_{60}^{n-}) = E_{\text{Madelung}} + E_{\text{BM}} - \frac{Z}{2}D(\text{C}_{60}^{n-} - \text{C}_{60}^{n-}). \quad (5)$$

The factor Z in the pair potential term denotes the coordination number of the C₆₀ molecules, which is 12 in the close-packed fcc structure and 8 in the bcc structure; E_{BM} denotes the Born-Mayer-type repulsive energy.

The formation of intercalation compounds is driven by a large gain in Madelung energy. We consider a complete charge transfer between the intercalants and the C₆₀ clusters, in agreement with *ab initio* results of Refs. 11 and 12 for the alkali compounds. We express the Madelung energy per unit cell as

$$E_{\text{Madelung}} = -\alpha q^2/a. \quad (6)$$

Here, q is the charge on the intercalant and a is the lattice constant of the conventional cubic unit cell. The Madelung constants for the different structures have been evaluated using the Ewald method. Our values are in agreement with previous results^{9,10} and are listed in Table III. Note that the Madelung constants for A₃C₆₀ and A₆C₆₀ are extremely large when compared to the AC₆₀ compound. This fact is mainly due to the large number of neighboring counter ions for each C₆₀ cluster.

The gain in Madelung energy is only partly compensated by the (mainly) closed-shell repulsion between the A⁺ and the C₆₀³⁻ ions in the lattice. An accurate knowledge of this repulsive interaction is necessary since it affects not only the cohesive energy, but also the equilibrium structure and compressibility of the bulk compounds. We model this closed-shell repulsion energy E_{BM} by pairwise Born-Mayer-type repulsive potentials

$V_{ij}^{\text{BM}}(r)$ (Ref. 28) as

$$E_{\text{BM}} = \sum_{i < j} V_{ij}^{\text{BM}}(r). \quad (7)$$

The pairwise potentials have been parametrized as²⁸

$$V_{ij}^{\text{BM}}(r) = a_{ij}e^{-\frac{r}{\rho}}, \quad (8)$$

where

$$a_{ij} = b \left(1 + \frac{z_i}{n_i} + \frac{z_j}{n_j} \right) e^{\frac{r_i+r_j}{\rho}}. \quad (9)$$

Here, z_i and z_j are the valences of the two interacting ions, n_i and n_j are the numbers of valence electrons in the outer shells of the ions, and r_i and r_j are the ionic radii. The valences have negative signs for electronegative ions. We use $n = 8$ for all simple ions except for Li where we use $n = 2$. We neglect the z/n term at the C₆₀ sites due to the large number of valence electrons on the C₆₀ molecule. We use $\rho = 0.345$ Å for the characteristic length of the Born-Mayer repulsion across the whole Periodic Table.²⁸ For ion pairs containing a C₆₀ molecule corresponding to the index j in Eq. (9), we use $r_j = r(\text{C}_{60})$ and express b as $b = \bar{b} \exp[-r(\text{C}_{60})/\rho]$. We determine the value of \bar{b} using the observed structural and elastic properties of K₃C₆₀ (Ref. 29) and find $\bar{b} = 1.76 \times 10^5$ eV. We find that this value of b fits the properties of Rb₃C₆₀,^{29,30} and use it for all other intercalation compounds as well. In Eq. (7) we only consider repulsive interactions between the C₆₀ sites and the neighboring intercalant ions. We find that the non-Coulombic (mainly closed-shell) repulsion between the intercalant ions can be neglected due to their small ionic radii and large separations.³¹ Of course, the interionic Coulomb repulsion is taken care of in the Madelung energy.

Finally, the intercalated solid is further stabilized by attractive interactions between neighboring C₆₀³⁻ clusters, stemming from weakly overlapping valence orbitals and Van der Waals interactions. Again, we decompose these interactions energies into pairwise energies. In the A₃C₆₀ compound, the energy gain associated with attractive C₆₀-C₆₀ interactions is $6 D(\text{C}_{60}^{3-} - \text{C}_{60}^{3-})$. As discussed, the Coulomb repulsion part of this pairwise interaction is taken care of in the Madelung energy. In

TABLE II. Total electron affinity A_{tot} corresponding to the process $\text{C}_{60} + ne^- \rightarrow \text{C}_{60}^{n-}$.

Final-state configuration	C ₆₀ ⁻	C ₆₀ ²⁻	C ₆₀ ³⁻	C ₆₀ ⁶⁻	C ₆₀ ¹²⁻
A_{tot} (eV)	2.74 ^a	3.42	1.09	-24.65	-173.06

^aExperimental value of Ref. 21.

TABLE III. Madelung constants α for the structures considered in this publication.

Structure	α
$A^+C_{60}^-$	3.4951
$A_3^+C_{60}^{3-}$	22.1220
$A_6^+C_{60}^{6-}$	56.2670

this context, we note that the inhomogeneity in the induced charge on the surface of the C_{60} molecules does not change the crystal energy, since the corresponding interactions average to zero in the crystal. On the other hand, the extra charge on a C_{60} molecule, which itself has 240 valence electrons, has a negligible effect on the non-Coulombic part of the interaction between a pair of C_{60} molecules. Consequently, $D(C_{60}^{3-} - C_{60}^{3-}) \approx D(C_{60} - C_{60})$. This fact explains why ΔH_f^0 is not sensitive to $D(C_{60} - C_{60})$, as mentioned above. In the case of AC_{60} and A_3C_{60} , the pristine and the intercalated solids have the same structure. Then, the contribution of Van der Waals interactions between C_{60} molecules to ΔH_f^0 stemming from the first and the last step of the Born-Haber cycle will nearly cancel.

III. STRUCTURAL AND COHESIVE PROPERTIES OF FULLERITE INTERCALATION COMPOUNDS

The energies associated with the individual steps in the Born-Haber cycle depend sensitively on the equilibrium structure of the corresponding compounds. Especially, the large Madelung energies which stabilize the intercalated compounds are balanced by repulsive interactions which in turn are closely related to the elastic properties

of the compounds. In order to calculate these energies with adequate precision, we found it necessary to obtain accurate estimates of the equilibrium lattice constants and bulk moduli for all compounds of interest.

Pristine fullerite is a face-centered cubic solid at room temperature, with C_{60} occupying the Bravais lattice sites. The conventional cubic unit cell has a large lattice constant $a = 14.20 \text{ \AA}$.¹⁷ The lattice contains two types of interstitial sites, namely the smaller tetrahedral and the larger octahedral sites, which can be occupied by intercalants. There are two tetrahedral sites and one octahedral site per C_{60} in the lattice. Using $r_C = 0.92 \text{ \AA}$ for the atomic radius of carbon³² and 3.5 \AA for the radius of the C_{60} molecule, we find that the diameter of the larger octahedral cavity is $\approx 5.4 \text{ \AA}$ and that of the smaller tetrahedral cavity is $\approx 3.5 \text{ \AA}$. These large sizes guarantee that especially the octahedral cavity can host any element in the Periodic Table. In the alkali intercalated (and superconducting) A_3C_{60} compound,⁹ which is the most stable phase for the alkali systems, all octahedral and tetrahedral sites are filled. We found it instructive to compare formation energies in this compound to the AC_{60} phase with the NaCl structure, where the intercalants occupy only the octahedral sites. Upon prolonged exposure of fullerite to the intercalant metal vapor, a transition from the fcc A_3C_{60} phase to the saturated phase A_6C_{60} with the body-centered cubic structure is observed.³³ In this case, each C_{60} molecule is surrounded by 24 intercalant ions.

As in graphite intercalation compounds, the stability of each of these phases is determined by the energetics of electron transfer between the intercalant and the C_{60} . For a given element, this energetics is given by the relationship between the ionization potential and electron

(a) AC_{60}				(b) A_3C_{60}				(c) A_6C_{60}							
$A^+C_{60}^-$	$A_3^+C_{60}^{3-}$	$A_3^+C_{60}^{6-}$	$A_6^+C_{60}^{6-}$	Li	Be	O	F	Li	Be	O	F	Li	Be	O	F
Li	Be	O	F	Li	Be	O	F	Li	Be	O	F	Li	Be	O	F
$a=14.14 \text{ \AA}$	$a=13.97 \text{ \AA}$	$a=14.00 \text{ \AA}$	$a=14.16 \text{ \AA}$	$a=13.95 \text{ \AA}$	$a=13.34 \text{ \AA}$	$a=13.72 \text{ \AA}$	$a=14.27 \text{ \AA}$	$a=10.92 \text{ \AA}$	$a=10.11 \text{ \AA}$	$a=10.57 \text{ \AA}$	$a=11.28 \text{ \AA}$	$a=11.00 \text{ \AA}$	$a=10.16 \text{ \AA}$	$a=11.16 \text{ \AA}$	$a=11.91 \text{ \AA}$
$B=0.20 \text{ MBar}$	$B=0.27 \text{ MBar}$	$B=0.26 \text{ MBar}$	$B=0.20 \text{ MBar}$	$B=0.30 \text{ MBar}$	$B=0.74 \text{ MBar}$	$B=0.64 \text{ MBar}$	$B=0.26 \text{ MBar}$	$B=0.49 \text{ MBar}$	$B=1.86 \text{ MBar}$	$B=1.60 \text{ MBar}$	$B=0.43 \text{ MBar}$	$B=0.48 \text{ MBar}$	$B=1.83 \text{ MBar}$	$B=1.34 \text{ MBar}$	$B=0.30 \text{ MBar}$
$\Delta H_f^0 = 0.74 \text{ eV}$	$\Delta H_f^0 = 13.14 \text{ eV}$	$\Delta H_f^0 = 4.68 \text{ eV}$	$\Delta H_f^0 = 1.50 \text{ eV}$	$\Delta H_f^0 = -0.78 \text{ eV}$	$\Delta H_f^0 = 8.10 \text{ eV}$	$\Delta H_f^0 = 5.63 \text{ eV}$	$\Delta H_f^0 = 2.13 \text{ eV}$	$\Delta H_f^0 = -0.62 \text{ eV}$	$\Delta H_f^0 = 8.76 \text{ eV}$	$\Delta H_f^0 = 11.46 \text{ eV}$	$\Delta H_f^0 = 4.06 \text{ eV}$	$\Delta H_f^0 = -1.28 \text{ eV}$	$\Delta H_f^0 = 2.34 \text{ eV}$	$\Delta H_f^0 = 13.25 \text{ eV}$	$\Delta H_f^0 = 5.19 \text{ eV}$
Na	Mg	S	Cl	Na	Mg	S	Cl	Na	Mg	S	Cl	Na	Mg	S	Cl
$a=14.14 \text{ \AA}$	$a=13.97 \text{ \AA}$	$a=14.07 \text{ \AA}$	$a=14.23 \text{ \AA}$	$a=14.01 \text{ \AA}$	$a=13.38 \text{ \AA}$	$a=14.34 \text{ \AA}$	$a=14.96 \text{ \AA}$	$a=11.00 \text{ \AA}$	$a=10.16 \text{ \AA}$	$a=11.16 \text{ \AA}$	$a=11.91 \text{ \AA}$	$a=11.00 \text{ \AA}$	$a=10.16 \text{ \AA}$	$a=11.16 \text{ \AA}$	$a=11.91 \text{ \AA}$
$B=0.20 \text{ MBar}$	$B=0.27 \text{ MBar}$	$B=0.26 \text{ MBar}$	$B=0.19 \text{ MBar}$	$B=0.30 \text{ MBar}$	$B=0.72 \text{ MBar}$	$B=0.51 \text{ MBar}$	$B=0.19 \text{ MBar}$	$B=0.48 \text{ MBar}$	$B=1.83 \text{ MBar}$	$B=1.60 \text{ MBar}$	$B=0.33 \text{ MBar}$	$B=0.48 \text{ MBar}$	$B=1.83 \text{ MBar}$	$B=1.34 \text{ MBar}$	$B=0.30 \text{ MBar}$
$\Delta H_f^0 = -0.02 \text{ eV}$	$\Delta H_f^0 = 6.48 \text{ eV}$	$\Delta H_f^0 = 3.95 \text{ eV}$	$\Delta H_f^0 = 2.04 \text{ eV}$	$\Delta H_f^0 = -1.45 \text{ eV}$	$\Delta H_f^0 = 1.55 \text{ eV}$	$\Delta H_f^0 = 6.48 \text{ eV}$	$\Delta H_f^0 = 3.29 \text{ eV}$	$\Delta H_f^0 = -1.28 \text{ eV}$	$\Delta H_f^0 = 2.34 \text{ eV}$	$\Delta H_f^0 = 13.25 \text{ eV}$	$\Delta H_f^0 = 5.19 \text{ eV}$	$\Delta H_f^0 = -1.28 \text{ eV}$	$\Delta H_f^0 = 2.34 \text{ eV}$	$\Delta H_f^0 = 13.25 \text{ eV}$	$\Delta H_f^0 = 5.19 \text{ eV}$
K	Ca	Se	Br	K	Ca	Se	Br	K	Ca	Se	Br	K	Ca	Se	Br
$a=14.16 \text{ \AA}$	$a=13.98 \text{ \AA}$	$a=14.12 \text{ \AA}$	$a=14.28 \text{ \AA}$	$a=14.24 \text{ \AA}$	$a=13.47 \text{ \AA}$	$a=14.62 \text{ \AA}$	$a=15.26 \text{ \AA}$	$a=11.26 \text{ \AA}$	$a=10.28 \text{ \AA}$	$a=11.40 \text{ \AA}$	$a=12.16 \text{ \AA}$	$a=11.26 \text{ \AA}$	$a=10.28 \text{ \AA}$	$a=11.40 \text{ \AA}$	$a=12.16 \text{ \AA}$
$B=0.20 \text{ MBar}$	$B=0.27 \text{ MBar}$	$B=0.25 \text{ MBar}$	$B=0.19 \text{ MBar}$	$B=0.26 \text{ MBar}$	$B=0.70 \text{ MBar}$	$B=0.46 \text{ MBar}$	$B=0.16 \text{ MBar}$	$B=0.43 \text{ MBar}$	$B=1.76 \text{ MBar}$	$B=1.24 \text{ MBar}$	$B=0.30 \text{ MBar}$	$B=0.43 \text{ MBar}$	$B=1.76 \text{ MBar}$	$B=1.24 \text{ MBar}$	$B=0.30 \text{ MBar}$
$\Delta H_f^0 = -0.95 \text{ eV}$	$\Delta H_f^0 = 2.14 \text{ eV}$	$\Delta H_f^0 = 3.85 \text{ eV}$	$\Delta H_f^0 = 2.23 \text{ eV}$	$\Delta H_f^0 = -2.09 \text{ eV}$	$\Delta H_f^0 = -2.49 \text{ eV}$	$\Delta H_f^0 = 6.94 \text{ eV}$	$\Delta H_f^0 = 3.67 \text{ eV}$	$\Delta H_f^0 = -1.87 \text{ eV}$	$\Delta H_f^0 = -1.36 \text{ eV}$	$\Delta H_f^0 = 13.98 \text{ eV}$	$\Delta H_f^0 = 5.54 \text{ eV}$	$\Delta H_f^0 = -1.87 \text{ eV}$	$\Delta H_f^0 = -1.36 \text{ eV}$	$\Delta H_f^0 = 13.98 \text{ eV}$	$\Delta H_f^0 = 5.54 \text{ eV}$
Rb	Sr	Te	I	Rb	Sr	Te	I	Rb	Sr	Te	I	Rb	Sr	Te	I
$a=14.17 \text{ \AA}$	$a=13.98 \text{ \AA}$	$a=14.24 \text{ \AA}$	$a=14.38 \text{ \AA}$	$a=14.41 \text{ \AA}$	$a=13.54 \text{ \AA}$	$a=15.15 \text{ \AA}$	$a=15.80 \text{ \AA}$	$a=11.43 \text{ \AA}$	$a=10.37 \text{ \AA}$	$a=11.83 \text{ \AA}$	$a=12.56 \text{ \AA}$	$a=11.43 \text{ \AA}$	$a=10.37 \text{ \AA}$	$a=11.83 \text{ \AA}$	$a=12.56 \text{ \AA}$
$B=0.20 \text{ MBar}$	$B=0.27 \text{ MBar}$	$B=0.24 \text{ MBar}$	$B=0.18 \text{ MBar}$	$B=0.24 \text{ MBar}$	$B=0.68 \text{ MBar}$	$B=0.39 \text{ MBar}$	$B=0.13 \text{ MBar}$	$B=0.40 \text{ MBar}$	$B=1.72 \text{ MBar}$	$B=1.30 \text{ MBar}$	$B=0.26 \text{ MBar}$	$B=0.40 \text{ MBar}$	$B=1.72 \text{ MBar}$	$B=1.30 \text{ MBar}$	$B=0.26 \text{ MBar}$
$\Delta H_f^0 = -1.16 \text{ eV}$	$\Delta H_f^0 = 0.78 \text{ eV}$	$\Delta H_f^0 = 4.09 \text{ eV}$	$\Delta H_f^0 = 2.70 \text{ eV}$	$\Delta H_f^0 = -2.12 \text{ eV}$	$\Delta H_f^0 = -3.63 \text{ eV}$	$\Delta H_f^0 = 8.01 \text{ eV}$	$\Delta H_f^0 = 4.31 \text{ eV}$	$\Delta H_f^0 = -1.89 \text{ eV}$	$\Delta H_f^0 = -2.29 \text{ eV}$	$\Delta H_f^0 = 15.48 \text{ eV}$	$\Delta H_f^0 = 6.15 \text{ eV}$	$\Delta H_f^0 = -1.89 \text{ eV}$	$\Delta H_f^0 = -2.29 \text{ eV}$	$\Delta H_f^0 = 15.48 \text{ eV}$	$\Delta H_f^0 = 6.15 \text{ eV}$
Cs	Ba			Cs	Ba			Cs	Ba			Cs	Ba		
$a=14.20 \text{ \AA}$	$a=14.00 \text{ \AA}$			$a=14.69 \text{ \AA}$	$a=13.70 \text{ \AA}$			$a=11.69 \text{ \AA}$	$a=10.56 \text{ \AA}$			$a=11.69 \text{ \AA}$	$a=10.56 \text{ \AA}$		
$B=0.20 \text{ MBar}$	$B=0.26 \text{ MBar}$			$B=0.21 \text{ MBar}$	$B=0.64 \text{ MBar}$			$B=0.36 \text{ MBar}$	$B=1.61 \text{ MBar}$			$B=0.36 \text{ MBar}$	$B=1.61 \text{ MBar}$		
$\Delta H_f^0 = -1.41 \text{ eV}$	$\Delta H_f^0 = -0.50 \text{ eV}$			$\Delta H_f^0 = -2.10 \text{ eV}$	$\Delta H_f^0 = -4.41 \text{ eV}$			$\Delta H_f^0 = -1.88 \text{ eV}$	$\Delta H_f^0 = -2.66 \text{ eV}$			$\Delta H_f^0 = -1.88 \text{ eV}$	$\Delta H_f^0 = -2.66 \text{ eV}$		

FIG. 2. Predicted equilibrium lattice constant a , bulk modulus B , and formation enthalpy ΔH_f^0 for different C_{60} fullerite intercalation compounds A_nC_{60} . Three different stoichiometries are considered: (a) A_1C_{60} (fcc structure), (b) A_3C_{60} (fcc structure), and (c) A_6C_{60} (bcc structure). Results are presented for elements A from the IA, IIA, VIA, and VIIA groups of the Periodic Table.

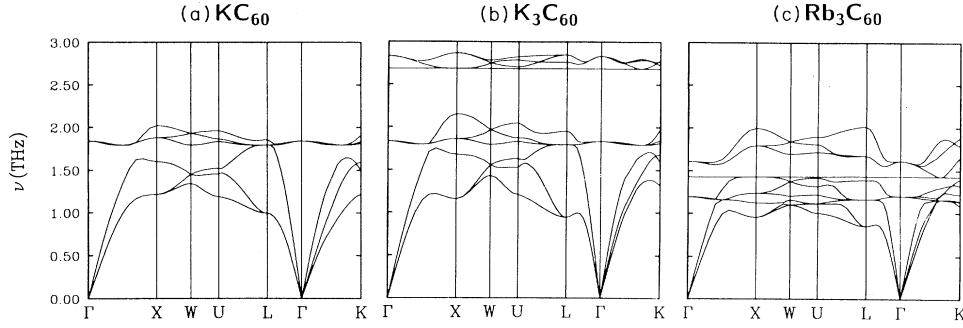


FIG. 3. Phonon band structure of (a) KC_{60} , (b) K_3C_{60} , and (c) Rb_3C_{60} .

affinity of the intercalant atom and the C_{60} molecule, respectively. As we discussed in Sec. II, C_{60} can act both as electron donor and electron acceptor. Consequently, both acceptor and donor elements can, in principle, be intercalated in fullerite. We investigate donor intercalants from groups IA and IIA and acceptor intercalants from groups VIA and VIIA and summarize our results in Fig. 2.

We determine the equilibrium lattice constant a of the compound by maximizing the cohesive energy of the intercalated solid with respect to the isolated ions, $E_{\text{coh}}(A_n^+C_{60}^{n-})$ (or the corresponding acceptor compound), using the expression in Eq. (5). The bulk modulus B is obtained from the second derivative of $E_{\text{coh}}(a)$ with respect to a in the equilibrium geometry. The distance dependence of $D(C_{60}-C_{60})$, E_{Madelung} , and E_{BM} in the intercalated solid has been discussed in Eqs. (4), (6), and (7), respectively. Since both a and B are of intrinsic interest, they are also listed in Fig. 2 for all the intercalation compounds we investigated.

Once the equilibrium structure and the elastic behavior of the intercalated compounds are known, the phonon spectra can be calculated by constructing the dynamical matrix. These phonon spectra are important in the determination of relevant phonon modes which can couple conduction electrons and lead to superconductivity.³⁴ In

Fig. 3 we present the phonon band structure of KC_{60} , K_3C_{60} , and Rb_3C_{60} along the high-symmetry lines in the Brillouin zone. The corresponding phonon density of states for the superconducting compound K_3C_{60} (Ref. 3) is shown in Fig. 4. The calculated phonon spectrum is characterized by low-lying C_{60} -derived acoustic modes which show little or no hybridization with high-frequency alkali-derived optical modes, which can be understood as Einstein modes.

From our results in Fig. 2 we conclude that the lattice constant a increases with increasing atomic number of the intercalant within the same group. The decrease of a when comparing neighboring alkali and alkaline-earth elements is due to the larger Madelung energy in the divalent donor-based solid. A similar trend is found when comparing neighboring group-VIA and group-VIIA elements, where group-VIA-based compounds have the smaller lattice constant. We find intercalant-induced changes of the lattice constant to be relatively moderate due to the large size of the interstitial sites in fullerite. Opposite and much more pronounced trends as for the lattice constant are found for the bulk modulus B . The main reason for this fact is the strongly anharmonic interionic repulsive interaction which leads to stiffer bonds at smaller values of the lattice constant.

The most important information which comes from our calculations is the formation energy ΔH_f^0 of intercalated fullerite. As seen from our results in Fig. 2, we expect only alkali and heavy alkaline-earth elements to form stable fullerite intercalation compounds, indicated by the negative sign of ΔH_f^0 . As we discuss in the following section, the trends across the Periodic Table can be understood from the delicate balance between the Madelung energy, ionization potentials, and electron affinities of the intercalant atoms.

IV. DISCUSSION

The results for the formation enthalpies, presented in Fig. 2, can be interpreted as resulting from several trends across the Periodic Table. The heats of formation are dominated by the Madelung energy which, for a given group, does not change significantly due to only moderate changes of the lattice constant. More important are the changes of the ionization potential and electron

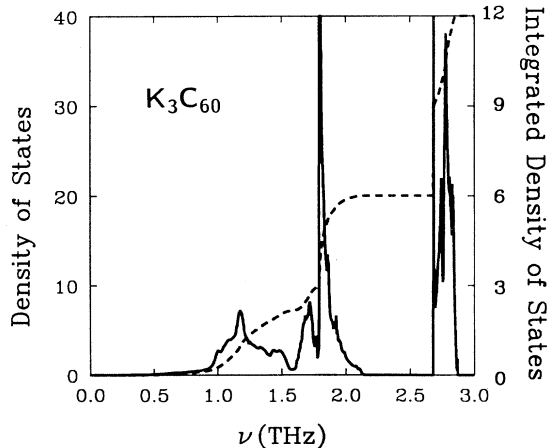


FIG. 4. Phonon density of states (solid line) and integrated density of states (dashed line) of K_3C_{60} .

affinity between elements in the same group which enter in the second step of the Born-Haber cycle, shown in Fig. 1. Due to the decreasing ionization potential of groups-IA and -IIA elements with increasing atomic number, the heavier elements get ionized more easily. This is reflected in larger absolute values for the reaction enthalpies, which are indicative of a strongly exothermic intercalation process, in agreement with the experimental trends.^{3,4} An analogous decrease of the electron affinity with increasing atomic number occurs in groups VIA and VIIA. The heavier intercalants are less likely to accept electrons and are consequently less reactive. This leads to an increasingly endothermic behavior during the intercalation process of heavy group-VIA and -VIIA elements.

We assume that group-IIA elements are doubly ionized which is more difficult to achieve than the single ionization of their alkali neighbors. This results in a smaller energy gain (or even a loss) during the intercalation process. For the acceptor elements, attachment of two electrons in the VIA group is much more difficult than of a single electron in the halide neighbor, resulting in larger energy losses predicted for the intercalation of group-VIA elements as compared to group-VIIA elements.

A more detailed discussion of the formation enthalpies of fullerite intercalation compounds is presented, group by group, in the following subsections.

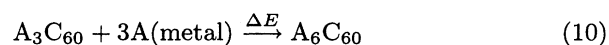
A. Group IA

In the most dilute system with the AC_{60} stoichiometry, only Li does not form a compound, mainly due to the large cohesive energy of the Li metal and the high ionization potential of the Li atom. Na has a smaller cohesive energy and a lower ionization potential than Li which makes the compound with NaCl structure marginally stable. The Na atom is much smaller than the interstitial sites and is likely to be in off-center geometry. The additional gain in Madelung energy (with respect to the high-symmetry geometry) is likely to further stabilize this compound. The radii of group-IA intercalant elements never exceed the size of the octahedral cavity, resulting in very small changes of the lattice constant and bulk modulus. On the other hand, the cohesive energies and atomic ionization potentials of alkali metals steadily decrease from K to Rb and Cs, which is reflected in the increased stability of the intercalation compounds with the heavier elements.

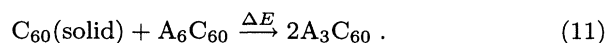
In the A_3C_{60} phase, all the alkali elements form stable intercalation compounds due to large Madelung energies. The calculated energy gain per atom in this phase is larger than in the AC_{60} phase, which is confirmed by the experimental observation that the A_3C_{60} phase does not decompose into AC_{60} and the pure metal. The occupation of the smaller tetrahedral sites in the A_3C_{60} phase makes these structures stiffer, which is reflected in a significantly larger bulk modulus. K_3C_{60} and Rb_3C_{60} are the most thoroughly investigated fullerite intercalation compounds to date.^{3,4,29,30,35,36} As we mentioned in Sec. II, the calculated repulsive interactions are based on the

observed lattice constant and bulk modulus of K_3C_{60} . We test our predictions in Rb_3C_{60} , where we find our predicted lattice constant $a = 14.41 \text{ \AA}$ to be in close agreement with the experimental value $a_{\text{expt}} = 14.49 \text{ \AA}$,^{29,30} and the predicted bulk modulus $B = 0.24 \text{ MBar}$ to be in similar agreement with the experimental value $B_{\text{expt}} = 0.22 \text{ MBar}$.²⁹

As shown in Fig. 2(c), all alkali compounds A_6C_{60} with the bcc structure are stable. This has been confirmed by the successful synthesis of the A_6C_{60} compounds, where $A = \text{Li, Na, K, Rb, and Cs}$.^{33,36-39} The observed insulating behavior of these compounds is easily understood by the complete filling of the t_{1u} orbital of the C_{60} molecules by six donor electrons. The bcc structure of the A_6C_{60} phase has a smaller packing fraction than the fcc lattice. There are only octahedral interstitial sites in this structure, three per C_{60} molecule, all of them filled by four alkali atoms (each alkali atom belongs to two neighboring octahedral sites). The intercalants are well separated from each other by a nearest-neighbor distance which is $\gtrsim 1 \text{ \AA}$ larger than the bond length in the alkali metal. As we mentioned before, the Born-Mayer repulsive energy between the intercalants is negligibly small in this geometry.³¹ The electrostatic attraction between the C_{60}^{6-} molecules and the large number of alkali counter ions reduces the distance between nearest-neighbor C_{60} molecules by $\approx 0.2 \text{ \AA}$ with respect to the value in pristine fullerite. We find the absolute value of the Madelung energy to be much larger in the A_6C_{60} than the A_3C_{60} phase, in spite of the strong Coulomb repulsion between four intercalant ions at the same octahedral site. The energy gain per intercalant atom in the A_6C_{60} phase is only slightly smaller than in the A_3C_{60} phase. The negative sign of ΔH_f^0 shows that the A_6C_{60} phase can be formed by intercalating A into the A_3C_{60} phase; the slightly smaller value of ΔH_f^0 indicates that A_6C_{60} is the saturated phase. We find the reaction



to be exothermic with $\Delta E = -4.95 \text{ eV}$ in the case of K, which indicates that A_6C_{60} will not decompose into A_3C_{60} and the metal A. On the other hand, one can speculate about the possibility of synthesizing the A_3C_{60} compound by mixing the pristine C_{60} solid and the saturated A_6C_{60} compound, as



In the case of K, we find this reaction to be exothermic with $\Delta E = -1.32 \text{ eV}$. This "back titration" is used as a well-defined synthesis process for K_3C_{60} (Ref. 29) and Rb_3C_{60} .³⁷ The bulk modulus of the A_6C_{60} alkali compounds is considerably larger than in the other phases since all interstitial sites are occupied by four intercalant atoms. We find our theoretical value for the lattice constant of K_6C_{60} , $a = 11.26 \text{ \AA}$, to be in close agreement with the experimental value $a_{\text{expt}} = 11.39 \text{ \AA}$.³³

B. Group IIA

We assume in our calculations that the group-IIA elements transfer both of their valence electrons to C₆₀ in the compound. We find that among these elements, only Ba is stable in the AC₆₀ phase. The lattice constant of alkaline-earth intercalation compounds is smaller than that of the comparable alkali compounds, mainly due to the larger value of the Madelung energy. This decrease of the lattice constant from group IA to group IIA is reflected in an increased bulk modulus B . As in the alkali compounds, we predict that the bulk modulus does not change from the heavy to the light intercalants.

In the A₃C₆₀ phase, we find the compounds of Ca, Sr, and Ba to be stable. The lattice constants decrease considerably as compared to the AC₆₀ phase, which is accompanied by a strong increase in B . Superconductivity at 8.4 K has been observed in Ca intercalated fullerite with simple cubic structure and the stoichiometry Ca₅C₆₀.⁵ Our predictions regarding stable phases of alkaline-earth-based compounds have been further confirmed by the recently observed stable phases of Sr and Ba compounds.⁴⁰

The alkaline-earth elements, which form stable A₃C₆₀ compounds, also form stable A₆C₆₀ compounds. The large difference of 11.5 eV between the formation enthalpies of the Be and the Ba compounds is mainly caused by the difference of 12.3 eV between the first and second ionization energies of these elements. Based on our calculated formation enthalpies for the A₃C₆₀ and A₆C₆₀ compounds we conclude that the A₃C₆₀ phase can be formed by an exothermic reaction from a mixture of pristine C₆₀ and A₆C₆₀, as indicated in Eq. (11). The strongly attractive Coulomb interactions reduce the lattice constant of the C₆₀ matrix substantially, more in the group-IIA than in the group-IA intercalation compounds. In the hypothetical Ca₆C₆₀ compound, the lattice constant is 0.98 Å smaller than in the corresponding compound of the neighboring element K; the corresponding reduction of the C₆₀-C₆₀ nearest-neighbor distance in the Ca compound is 0.85 Å. This closer packing is reflected in the bulk moduli. In the A₆C₆₀ phase, typical values of B are more than twice as large as those in the more dilute A₃C₆₀ phase, and comparable to metallic Fe.

As we pointed out above, the inability of Mg to form a stable intercalation compound is mainly due to its large first and second ionization potentials. At this point, it is instructive to speculate whether a stable compound could be formed based on Mg⁺. We have performed the calculations for the Born-Haber cycle of Mg_{*n*}⁺C₆₀^{*n*-} and compared the results to those for Na_{*n*}⁺C₆₀^{*n*-} and found that the equilibrium structures are very similar and most steps are energetically equivalent. The main difference between Na⁺ and Mg⁺ based compounds is the first ionization potential of the atoms, which is 7.65 eV for Mg and 5.14 eV for Na. This reduces the formation enthalpy of fullerite compounds based on monovalent Mg by 2.5 eV with respect to comparable Na compounds, and hence makes the Mg_{*n*}⁺C₆₀^{*n*-} compounds unstable. The only possibility for a Mg-based fullerite compound to be stable exists if the bonds between Mg intercalants and the

C₆₀ matrix are covalent. This seems to be confirmed by the recent synthesis of a Mg-based C₆₀ compound which has nonmetallic character.⁴⁰

In the following section, we will turn to acceptor intercalants, starting with the halide group.

C. Group VIIA

We find that none of the halide compounds are stable with respect to pure C₆₀ and the halide gas. In order to understand this fact, we compared the individual energies occurring in the Born-Haber cycles of alkali and halide compounds in the same row of the Periodic Table. We found that the energy associated with the first step, involving the vaporization of solid C₆₀ and dissociation of molecular halide, and the last step, namely the formation of the intercalation compound from the respective ions, are very similar for the different group-IA and -VIIA systems. The large difference occurs during the ionization step on the atomic level, as we can illustrate for the A₃C₆₀ compound. We find that the energy necessary to ionize an alkali atom is very similar to the energy gain associated with electron attachment to a halide atom. Yet the energy to triply ionize a C₆₀ cluster, $I = 34.96$ eV, is much larger than the energy gain when attaching three electrons to a C₆₀ molecule, $A = 1.09$ eV (see Tables I and II). The large ionization energy of C₆₀ enters the Born-Haber cycle for halide intercalation compounds, and hence can be viewed as the cause of their instability.

The arguments used to explain the positive value of the formation enthalpy ΔH_f^0 in the A₃C₆₀ halide phase apply also to the AC₆₀ and A₆C₆₀ phases. The stability of alkali compounds and the instability of halide compounds can again be explained by comparing the vastly different total ionization potentials and electron affinities of the C₆₀ cluster for the given ionic final state, which are given in Tables I and II.

The variation of the formation enthalpy between the light and the heavy halides has two origins. First, the light halides have a larger electron affinity which results in the stabilization of the compound. Second, the lattice constant a decreases from the heavy towards the light elements, resulting in a larger Madelung energy gain during the formation of the solid from the ions. The decrease of a with decreasing atomic number is accompanied by a strong increase of the bulk modulus. There are two counteracting trends which change the lattice constant from the AC₆₀ to the A₃C₆₀ phase. As our results in Fig. 2 indicate, the lattice expansion due to the large halide ions occupying the smaller tetrahedral sites in the A₃C₆₀ lattice is partly compensated by the Madelung energy gain during lattice contraction. This still applies in the hypothetical A₆C₆₀ phase, where the lattice constant is significantly smaller than in the A₃C₆₀ compounds, mainly due to the Madelung energy gain associated with lattice contraction. This lattice contraction is again reflected in the large increase of the bulk modulus in the A₆C₆₀ phase as compared to the A₃C₆₀ phase. Still, the bulk moduli of halide intercalated compounds are well below

those of comparable alkali compounds, mainly due to the larger compressibility of the halide ions.

The arguments for the stability of halide intercalation compounds apply, of course, only to the structures studied in this paper. Other possible structures we can think of could contain endohedrals or halide molecules. The latter possibility has been confirmed recently, when varying amounts of I_2 have been found in C_{60} following exposure to iodine.^{41,42} Fluorine atoms, on the other hand, tend to form covalent bonds with C_{60} , giving rise to a different type of compound based on fluorinated fullerenes such as $C_{60}F_{36}$.⁴³

D. Group VIA

Our results in Fig. 2 indicate that group-VIA elements, the same as group-VIIA elements, do not form stable intercalation compounds. Free doubly charged group-VIA A^{2-} ions are known to be unstable.⁴⁴ Since no reasonable estimate is available for the second electron affinity of these ions,⁴⁵ we simply assume the second electron affinity to be the same as the first electron affinity. When used in the Born-Haber cycle, this value gives the lower limit of the formation enthalpy of the compound. The positive values for ΔH_f^0 which we find for all group-VIA elements are again to be blamed mainly on the large ionization potential of the C_{60} molecule, which dominates over the increased Madelung energy due to the larger charge of the acceptor ions. Again, our results only apply to the three hypothetical geometries we studied here. We cannot exclude the existence of other different group-VIA-based intercalation compounds, such as compounds containing intercalant molecules. As for group-VIIA elements, the variations in ΔH_f^0 within the VIA group are linked with variations of the lattice constant of the compound and changes of the electron affinity of the elements. We find the trends in the structural properties (a , B) of group-VIA-based compounds to closely follow those found in group VIIA intercalation compounds.

E. Phonon spectra and superconductivity

One of the most important properties of intercalated fullerite is superconductivity, which has been observed in many alkali intercalation compounds with the A_3C_{60} stoichiometry.^{3,4,6} The observed nonzero isotope effect⁴⁶ in these compounds makes the electron-phonon coupling mechanism a likely candidate for the pairing of electrons. Reliable phonon spectra are an essential prerequisite for the resolution of the remaining uncertainties regarding the important phonon modes which are responsible for superconductivity in these compounds.³⁴ Our results for the phonon spectra of KC_{60} , K_3C_{60} , and Rb_3C_{60} are shown in Figs. 3 and 4.

The phonon spectra consist of low-lying C_{60} -derived acoustic modes which are well separated from high-frequency optical modes due to the alkali intercalants. The latter modes have low dispersion and can be interpreted as Einstein modes. The frequency of the optical modes increases with increasing stiffness of the interac-

tion potential between the alkali atom, acting as an Einstein oscillator, and the matrix. For a given intercalant A , this frequency is expected to be lower in the AC_{60} structure, where only the octahedral sites are filled, than in the A_3C_{60} structure, which contains occupied tetrahedral sites. In the latter case, we expect two optical bands, one due to octahedral sites at a frequency comparable to AC_{60} , and the other at a much higher frequency due to alkali atoms in tetrahedral sites. This is clearly the case for the optical modes at $\nu = 1.8$ THz (due to octahedral K) and at $\nu = 2.7$ THz (due to tetrahedral K) in KC_{60} and K_3C_{60} , as shown in Figs. 3(a) and 3(b). Figure 3(c) reflects the fact that the bonding in Rb_3C_{60} and K_3C_{60} are similar. The comparison of the corresponding spectra indicates that the optical modes of alkali atoms are reduced in frequency according to the large 2:1 mass ratio between Rb and K. The acoustic C_{60} -derived part of the spectrum is much less affected by the change from K to Rb.

The absence of hybridization between the alkali and the C_{60} -derived modes has also been predicted previously by Zhang, Zheng, and Bennemann,¹⁰ albeit due to different physics. Our results indicate that in the equilibrium geometry of K_3C_{60} , the K- C_{60} bonds are compressed in the tetrahedral sites, while the C_{60} - C_{60} bonds are stretched. The stiff K- C_{60} interaction potentials—especially in the tetrahedral sites—push the corresponding Einstein modes above the highest C_{60} -derived acoustic modes, hence suppressing hybridization. The calculation in Ref. 10 is based on the simplifying assumption that *all* individual bonds in the lattice are relaxed. The consequence of this model is a suppressed hybridization between the K-derived optical and C_{60} -derived acoustic modes in spite of the fact that the Einstein modes due to tetrahedral K atoms are predicted¹⁰ to lie in the frequency range of C_{60} fullerite.

V. SUMMARY AND CONCLUSIONS

We have predicted $T = 0$ K formation enthalpies of donor and acceptor-based C_{60} fullerite intercalation compounds with the AC_{60} , A_3C_{60} , and A_6C_{60} stoichiometries based on a thermodynamic Born-Haber cycle. Energies associated with the individual steps in the cycle have been carefully estimated using available experimental and theoretical data. The corresponding calculations provide details of the structure, lattice constant, and the bulk modulus of the intercalation compounds.

We have evaluated and listed the corresponding structural and elastic data together with the predicted formation enthalpies for groups IA, IIA, VIA, and VIIA of the Periodic Table. Phonon spectra, available from our total-energy calculations, are presented for selected alkali intercalation compounds which show superconducting behavior.

Our results indicate that alkali elements form stable fullerite intercalation compounds. We found alkaline-earth elements Ca, Sr, and Ba to be the most prominent candidates for intercalation. The corresponding calculations for acceptor intercalants indicate that none of

the group-VIA and -VIIA-based ionic intercalation compounds is stable with respect to solid C₆₀ and the intercalant in the standard form. Our results, however, do not address the possibility of intercalating molecules, or modifying the C₆₀ matrix in a chemical reaction.

The usefulness of our approach to estimate formation enthalpies can ultimately only be judged by corresponding experiments. We also hope that future experiments can reduce the uncertainty regarding some of the quantities used in the Born-Haber cycle, such as the higher electron affinities and ionization potentials of C₆₀ molecules, and equilibrium structures, lattice constants, and bulk

moduli of the compounds. We have also successfully applied the Born-Haber cycle method to calculate the formation enthalpy of lanthanide and actinide compounds, a new class of potential C₆₀-based superconductors,⁴⁷ and to endohedral molecules such as K-C₆₀ complexes. Our results for the stabilities of endohedral complexes will be presented separately.⁴⁸

ACKNOWLEDGMENTS

The authors acknowledge useful discussions with Aurel Bulgac. This research was supported by the National Science Foundation under Grant No. PHY-8920927.

- ¹W. Krätschmer, L.D. Lamb, K. Fostiropoulos, and D.R. Huffman, *Nature* **347**, 354 (1990).
- ²H.W. Kroto, J.R. Heath, S.C. O'Brien, R.F. Curl, and R.E. Smalley, *Nature* **318**, 162 (1985).
- ³A.F. Hebard, M.J. Rosseinsky, R.C. Haddon, D.W. Murphy, S.H. Glarum, T.T.M. Palstra, A.P. Ramirez, and A.R. Kortan, *Nature* **350**, 600 (1991).
- ⁴M.J. Rosseinsky, A.P. Ramirez, S.H. Glarum, D.W. Murphy, R.C. Haddon, A.F. Hebard, T.T.M. Palstra, A.R. Kortan, S.M. Zahurak, and A.V. Makhija, *Phys. Rev. Lett.* **66**, 2830 (1991); M.J. Rosseinsky, D.W. Murphy, R.M. Fleming, R. Tycko, A.P. Ramirez, T. Siegrist, G. Dabbagh, and S.E. Barrett, *Nature* **356**, 416 (1992); Stephen P. Kelty, Chia-Chun Chen, and Charles M. Lieber, *ibid.* **352**, 223 (1991); K. Tanigaki, I. Hirosawa, T.W. Ebbesen, J. Mizuki, Y. Shimakawa, Y. Kubo, J.S. Tsai, and S. Kuroshima, *ibid.* **356**, 419 (1992).
- ⁵A.R. Kortan, N. Kopylov, S. Glarum, E.M. Gyorgy, A.P. Ramirez, R.M. Fleming, F.A. Thiel, and R.C. Haddon, *Nature* **355**, 529 (1992).
- ⁶K. Tanigaki, T.W. Eddesen, S. Saito, J. Mizuki, J.S. Tsai, Y. Kubo, and S. Kuroshima, *Nature* **352**, 222 (1991).
- ⁷For a review see K.C. Hass, in *Solid State Physics*, edited by H. Ehrenreich and D. Turnbull (Academic, Orlando, 1989), Vol. 42.
- ⁸For reviews, see *Graphite Intercalation Compounds I*, edited by H. Zabel and S.A. Solin, Springer Series in Materials Science Vol. 14 (Springer-Verlag, New York, 1990); M.S. Dresselhaus and G. Dresselhaus, *Adv. Phys.* **30**, 139 (1981).
- ⁹R.M. Fleming, M.J. Rosseinsky, A.P. Ramirez, D.W. Murphy, J.C. Tully, R.C. Haddon, T. Siegrist, R. Tycko, S.H. Glarum, P. Marsh, G. Dabbagh, S.M. Zahurak, A.V. Makhija, and C. Hampton, *Nature* **352**, 701 (1991).
- ¹⁰W. Zhang, H. Zheng, and K.H. Bennemann, *Solid State Commun.* (to be published).
- ¹¹J.L. Martins and N. Troullier, *Phys. Rev. B* **46**, 1766 (1992).
- ¹²Susumu Saito and Atsushi Oshiyama, *Phys. Rev. B* **44**, 11 536 (1991). The value quoted has been obtained using the experimental cohesive energy of metallic K, $E_{\text{coh}}(\text{K})=0.934$ eV, and of fullerite, $E_{\text{coh}}(\text{C}_{60})=1.6$ eV. The latter value is a theoretical result obtained in the same reference.
- ¹³C. Kittel, *Introduction to Solid State Physics*, 6th ed. (Wiley, New York, 1986), p. 55.
- ¹⁴*CRC Handbook of Chemistry and Physics*, 70th ed. (CRC, Boca Raton, FL, 1990), p. E-80.
- ¹⁵H. Hotop and W.C. Lineberger, *J. Phys. Chem. Ref. Data* **14**, 731 (1985).
- ¹⁶Susumu Saito and Atsushi Oshiyama, *Phys. Rev. Lett.* **66**, 2637 (1991).
- ¹⁷J.H. Weaver, J.L. Martins, T. Komeda, Y. Chen, T.R. Ohno, G.H. Kroll, N. Troullier, R.E. Haufler, and R.E. Smalley, *Phys. Rev. Lett.* **66**, 1741 (1991).
- ¹⁸Yang Wang, D. Tománek, and G.F. Bertsch, *Phys. Rev. B* **44**, 6562 (1991).
- ¹⁹Steven J. Duclos, Keith Brister, R.C. Haddon, A.R. Kortan, and F.A. Thiel, *Nature* **351**, 380 (1991).
- ²⁰J. Abrefah, D.R. Orlander, M. Balooch, and W.J. Siekhaus, *Appl. Phys. Lett.* **60**, 1313 (1992).
- ²¹S.H. Yang, C.L. Pettiette, J. Conceicao, O. Chesnovsky, and R.E. Smalley, *Chem. Phys. Lett.* **139**, 233 (1987).
- ²²I.V. Hertel, H. Steger, J. de Vries, B. Weisser, C. Menzel, B. Kamke, and W. Kamke, *Phys. Rev. Lett.* **68**, 784 (1992).
- ²³H. Steger, J. de Vries, B. Kamke, W. Kamke, and T. Drewello, *Chem. Phys. Lett.* **194**, 452 (1992).
- ²⁴C.W. Walter, Y.K. Bae, D.C. Lorents, and J.R. Peterson, *Chem. Phys. Lett.* **195**, 543 (1992).
- ²⁵C. Lifshitz, M. Iraqi, T. Peres, and J.E. Fischer, *Int. J. Mass Spectrom. Ion Processes* **107**, 565 (1991).
- ²⁶R.L. Hettich, R.N. Compton, and R.H. Ritchie, *Phys. Rev. Lett.* **67**, 1242 (1991).
- ²⁷W. Walter (private communication).
- ²⁸F. Seitz, *Modern Theory of Solids*, 1st ed. (McGraw Hill, New York, 1940), p. 82.
- ²⁹O. Zhou, G.B.M. Vaughan, Q. Zhu, J.E. Fischer, P.A. Heiney, N. Coustel, J.P. McCauley, Jr., and A.B. Smith III, *Science* **255**, 833 (1992).
- ³⁰Q. Zhu, O. Zhou, N. Coustel, G. Vaughan, J.P. McCauley, Jr., W.J. Romanow, J.E. Fischer, and A.B. Smith III, *Science* **254**, 545 (1991).
- ³¹We estimate the repulsive energy between two intercalant sites using the many-body alloy Hamiltonian [D. Tománek and K.H. Bennemann, *Surf. Sci.* **163**, 503 (1985); D. Tománek, *Phys. Lett.* **113A**, 445 (1986); D. Tománek, S. Mukherjee, and K.H. Bennemann, *Phys. Rev. B* **28**, 665 (1983); **29**, 1076(E) (1984); D. Tománek, A.A. Aligia, and C.A. Balseiro, *ibid.* **32**, 5051 (1985); W. Zhong, Y.S. Li, and D. Tománek, *ibid.* **44**, 13 053 (1991)]. At the closest interionic distance, which is found in A₆C₆₀, the pair interaction energy is ≈ 0.02 eV and can be safely neglected when compared to the other energy terms.
- ³²C. Kittel, *Introduction to Solid State Physics*, 6th ed. (Ref. 13), p. 76.
- ³³O. Zhou, J.E. Fischer, N. Coustal, S. Kycia, O. Zhu, A.R.

- McGhie, W.J. Romanow, J.P. McCauley, Jr., A.B. Smith, and D.E. Cox, *Nature* **351**, 462 (1991).
- ³⁴J.L. Martins, N. Troullier, and M. Schnabel (unpublished); G. Baskaran and E. Tosatti, *Curr. Sci.* **61**, 33 (1991); F.C. Zhang, M. Ogata, and T.M. Rice, *Phys. Rev. Lett.* **67**, 3452 (1991); I.I. Mazin, S.N. Rashkeev, V.P. Antropov, O. Jepsen, A.I. Liechtenstein, and O.K. Andersen (unpublished); C.M. Varma, J. Zaanen, and K. Raghavachari, *Science* **254**, 989 (1991); M. Schluter, M. Lannoo, M. Needels, G.A. Baraff, and D. Tománek, *Phys. Rev. Lett.* **68**, 526 (1992).
- ³⁵P.J. Benning, D.M. Poirier, T.R. Ohno, Y. Chen, M.B. Jost, F. Stepniak, G.H. Kroll, J.H. Weaver, J. Fure, and R.E. Smalley, *Phys. Rev. B* **45**, 6899 (1992).
- ³⁶C. Gu, F. Stepniak, D.M. Poirier, M.B. Jost, P.J. Benning, Y. Chen, T.R. Ohno, J.L. Martin, J.H. Weaver, J. Fure, and R.E. Smalley, *Phys. Rev. B* **45**, 6348 (1992).
- ³⁷J.P. McCauley, Q. Zhu, N. Coustel, O. Zhou, G. Vaughan, S.H.J. Idziak, J.E. Fischer, S.W. Tozer, D.M. Groski, N. Bykovetz, C.L. Lin, A.R. McGhie, B.H. Allen, W.J. Romanow, A.M. Denenstien, and A.B. Smith III, *J. Am. Chem. Soc.* **113**, 8537 (1991).
- ³⁸Ying Wang, J.M. Holden, A.M. Rao, Wen-Tse Lee, G.T. Hager, X.X. Bi, S.L. Ren, G.W. Lehman, and P.C. Eklund (unpublished).
- ³⁹S.J. Duclos, R.C. Haddon, S. Glarum, A.F. Hebard, and K.B. Lyons, *Science* **254**, 1625 (1991).
- ⁴⁰Y. Chen, F. Stepniak, J.H. Weaver, L.P.F. Chibante, and R.E. Smalley, *Phys. Rev. B* **45**, 8845 (1992).
- ⁴¹T.R. Ohno, G.H. Kroll, and J.H. Weaver, L.P.F. Chibante, and R.E. Smalley, *Nature* **355**, 401 (1991).
- ⁴²Q. Zhu, D.E. Cox, J. E. Fischer, K. Kniaz, A.R. McGhie, and O. Zhou, *Nature* **355**, 713 (1991).
- ⁴³H. Selig, C. Lifshitz, T. Peres, J.E. Fischer, A.B. Smith McGhie, W.J. Romanow, and J.P. McCauley, Jr., *J. Am. Chem. Soc.* **113**, 5475 (1991).
- ⁴⁴D. Spence, W.A. Chupka, and C.M. Stevens, *Phys. Rev. A* **26**, 654 (1982).
- ⁴⁵D.F.C. Morris, *J. Phys. Chem. Solids* **5**, 264 (1958).
- ⁴⁶T.W. Ebbesen, J.S. Tsai, K. Tanigaki, J. Tabuchi, Y. Shimakawa, Y. Kubo, I. Hirose, and J. Mizuki, *Nature* **355**, 620 (1992); A.P. Ramirez, A.R. Kortan, M.J. Rosseinsky, S.J. Duclos, A.M. Muzsca, R.C. Haddon, D.W. Murphy, A.V. Makhija, S.M. Zahurak, and K.B. Lyons, *Phys. Rev. Lett.* **68**, 1058 (1991); Chia-Chun Chen and Charles M. Lieber, *J. Am. Chem. Soc.* **114**, 3141 (1992).
- ⁴⁷Rodney S. Ruoff, Yang Wang, and David Tománek, *Chem. Phys. Lett.* **201** (1993).
- ⁴⁸Rodney S. Ruoff, David Tománek, and Yang Wang (unpublished).